Optics Letters

Brighter CARS hypermicroscopy via "spectral surfing" of a Stokes supercontinuum

J. G. Porquez, R. A. Cole, J. T. Tabarangao, and A. D. Slepkov*

Department of Physics & Astronomy, Trent University, 1600 W Bank Dr., Peterborough, Ontario, Canada
**Corresponding author: aaronslepkov@trentu.ca*

Received 29 March 2017; revised 10 May 2017; accepted 10 May 2017; posted 11 May 2017 (Doc. ID 291586); published 6 June 2017

We present a simple technique that significantly enhances the interaction of pump pulses with a supercontinuum Stokes generated by a particular nonlinear fiber for time-gated experiments such as coherent anti-Stokes Raman scattering (CARS). The enhancement is achieved through a synchronized power-tuning/time delay scheme that we call *spectral surfing*. In this Letter, we introduce spectral surfing and demonstrate how its application to an economical CARS hypermicroscopy scheme increases the brightness, contrast, and spectral scanning range, while potentially reducing sample light exposure.

OCIS codes: (180.4315) Nonlinear microscopy; (300.6230) Spectroscopy, coherent anti-Stokes Raman scattering; (320.6629) Supercontinuum generation; (170.5810) Scanning microscopy.

https://doi.org/10.1364/OL.42.002255

Coherent anti-Stokes Raman scattering (CARS) is a chemical-specific, label-free microscopy technique that shows growing potential for materials characterization and biomedical imaging [1–3]. A particular experimental approach to CARS, known as spectral focusing (SF), enables concurrent microscopy and spectroscopy (i.e., hypermicroscopy) by using broadband fs pulses and a single-element detector such as a photomultiplier tube [3–7]. SF-CARS utilizes chirped pump and Stokes pulses with a reduced instantaneous frequency difference (IFD) bandwidth [7,8] to yield improved CARS spectral resolutions for identifying compounds having multiple dense peaks, especially in the molecular fingerprint frequencies (<1800 cm^{-1}). The development and applications of SF-CARS, in tandem with multimodal imaging modalities such as two-photon excitation fluorescence (TPEF) and multi-harmonic generation, are garnering continued interest for materials science and biomedical imaging [3,4,6–9].

Since the development of CARS microscopy, applications have largely relied on the imaging of CH vibrational frequencies ($\sim$2800 cm^{-1}–3100 cm^{-1}) [1,10]. By contrast, important information in the dense fingerprint region ($\sim$500 cm^{-1}–1800 cm^{-1}) has received considerably less attention, largely due to experimental limitations. Recent advances in "multiplex CARS"—a related technique that uses spectrometers for anti-Stokes signal detection—have pushed CARS imaging applications to span the fingerprint-to-CH frequencies (500 cm^{-1}–3500 cm^{-1}) [11,12]. This now enables the identification of key cellular components such as DNA and lipids in a single hyperspectral scan [13].

In view of SF-CARS, wherein images can be acquired for a given chemical contrast at several frames per second, we have reported an experimental approach, capable of detecting molecular vibrations from 620–3150 cm^{-1} that utilizes a Stokes supercontinuum generated in a nonlinear photonic crystal fiber (PCF) [14] pumped by relatively long seed pulses (200 fs, 70 cm^{-1} full width at half-maximum [FWHM] bandwidths). As with multiplex CARS, SF-CARS is compatible with powerful phase retrieval methods that convert raw CARS spectra—reshaped by the nonresonant background—to spontaneous Raman-like spectra [13–16]. Thus, SF-CARS is an agile imaging technique capable of switching between imaging-first and spectrum-first quantitative microscopy.

Among various approaches to SF-CARS, PCF-based techniques have the advantage of being particularly economical. Furthermore, the large spectral bandwidth of the PCF-generated Stokes supercontinuum permits easy scanning of a wide range of CARS frequencies, thus adding spectroscopic agility. The main technical drawback of the approach, however, is that the Stokes supercontinuum generated by PCF sources is highly variable across its spectrum [14,16–18], yielding regions of Stokes wavelength with limited brightness.

In an effort to maximize the utility of PCFs for SF-CARS, their supercontinuum generation (SCG) characteristics must be improved. In general, the supercontinua generated in PCF sources, especially those with closely lying zero-dispersion wavelengths such as the commercially available FemtoWHITE CARS (FWCARS) module, are heavily dependent on seed pulse characteristics [17,18]. For example, the location of the spectral maximum of the output can be varied as a function of supercontinuum generating seed pulse power [14,19]. This dependence can be exploited for SF-CARS since, at any instant, only a portion of the supercontinuum is used to access a unique CARS frequency or IFD—which depends on the spectro-temporal overlap of the pump and Stokes pulses. Therefore, synchronizing the overlap timing of the pump pulse with the tunable Stokes supercontinuum at the desired IFD, can lead to an overall improvement of CARS brightness across the spectral scan range.

We term such synchronization "spectral surfing." Such active power tuning of PCF-borne Stokes light for increased CARS signals is conceptually similar to the soliton self-frequency shift approach to multiplex CARS by Andersen *et al.* [19], except that here we power-tune the supercontinuum well beyond the zero-dispersion point and utilize a much broader Stokes, without the need for wavelength scanning. As demonstrated in this Letter, with spectral surfing, we obtain increased CARS brightness, reduced light dosage, and an expanded spectral scanning range that spans 350 to 3500 cm^{-1} in a single scan with an oscillator operating at 800 nm.

Beyond applications to CARS hypermicroscopy, we anticipate that spectral surfing could also benefit various time-gated experiments, wherein sources can be tuned as a function of time such as in other four-wave mixing techniques, as well as optical coherence tomography experiments utilizing tunable broad-spectrum light sources [20,21].

A simple schematic of the key features of the experimental setup is shown in Fig. 1. A Ti:sapphire oscillator is configured to generate an 800 nm pump having a Gaussian FWHM bandwidth of 100 cm^{-1} (nominal pulse duration of 150 fs). Part of this beam is routed to a FWCARS SCG module (NKT Photonics), the output of which becomes the Stokes beam for CARS. The seed pulse intensity coupled to the SCG module is controlled using a motorized half-wave plate (HWP) followed by a Faraday isolator, together acting as a computer-controlled variable attenuator. The original 800 nm beam acts as degenerate pump and probe for CARS [1], and passes through a computerized time delay stage before being recombined with the Stokes beam at an angled dichroic mirror. Each arm passes through a fixed amount of high-dispersion glass for chirp-matching purposes. The combined beam is then routed to a customized laser-scanning microscope, as detailed previously [14].

The HWP and pump delay stage are synchronized according to both the CARS calibration and the spectral-surfing calibration functions. The CARS frequency calibration function, $\Omega_R(x)$, maps the delay stage position, x, into the equivalent Raman frequency, Ω_R. As shown previously, the CARS calibration function can be approximated by a (predominantly linear) second-order polynomial [14]. Any sample that can generate adequate four-wave mixing signals at the anti-Stokes frequency such as the glass coverslip, can be used as a calibration sample. The appropriate CARS frequency is determined by computing the frequency difference between the central frequency of the pump and the central frequency of the anti-Stokes signal, collected by a spectrometer in the transmitted direction. The CARS frequency calibration function is then synchronized with the computer-controlled HWP for spectral surfing.

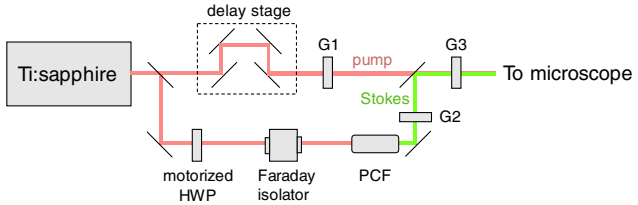

Fig. 1. Schematic of experimental layout of spectral-focusing CARS with a supercontinuum Stokes. The output of a Ti:sapphire oscillator is split into pump and Stokes beams. A Stokes supercontinuum is generated in a PCF. The supercontinuum seed pulse power is actively controlled by the combination of a motorized HWP and isolator. The chirps of the two beams are matched by blocks of SNPH-2 glass (G1, 25 mm; G2, 57 mm; G3, 101 mm).

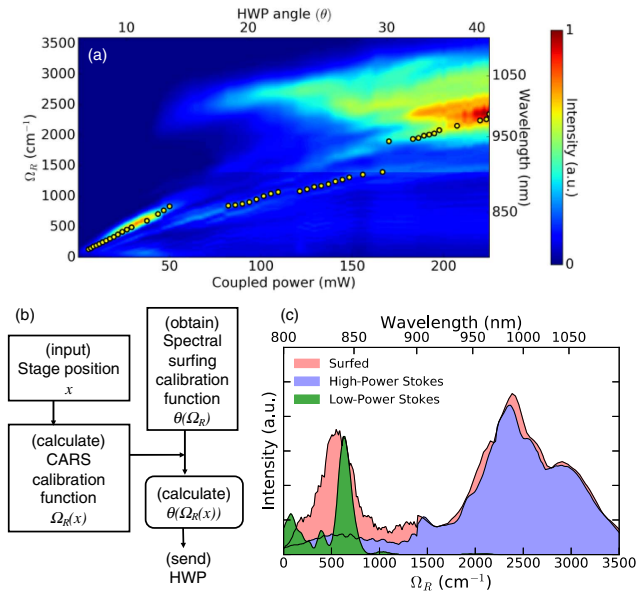

Fig. 2. Stokes supercontinuum power tuning and spectral surfing. (a) Stokes spectrum versus SCG seed power. The small circles correspond to points of maximum spectral intensity at unique IFD, Ω_R, which are then used to interpolate a spectral surfing calibration function, $\theta(\Omega_R)$. (b) Block algorithm for spectral surfing used to dynamically control the Stokes supercontinuum for CARS. (c) Stokes supercontinuum generated by "low" (37 mW, green) and "high" (220 mW, blue) coupled seed power, and the overall trace of the power-tuning sequence representing the effective "surfed" spectrum (red). Visualization 1 shows an animated version of (c).

The supercontinuum generated by PCFs often contains spectral components at both shorter and longer wavelengths than the pump. For CARS microscopy purposes, it is typically the longer-wavelength components that are used as broadband Stokes light. The red-shifted continuum generated by the FWCARS module is shown in Fig. 2(a), plotted as IFD and, thus, the vibrational frequency probed, Ω_R, against both the PCF-coupled seed power and the HWP angle. For each coupled power (or HWP angle), a Stokes supercontinuum having a spectral maximum at a particular wavelength can be generated. These are *points of maximum spectral intensity* that can be overlapped temporally with the pump beam for a maximized CARS signal (or any other time-gated cross-phase modulation process).

Because in SF-CARS a narrow range of IFDs are probed at a given moment in time, given by the timing of the pump delay stage, the Stokes can be optimized to maximize CARS intensity by utilizing the information obtained from the *points of maximum spectral intensity*. This method of dynamically tuning the SCG to maximize the signal in a time-gated experiment is what we call spectral surfing, in reference to the notion that one is synchronizing the interaction with a monotonically moving spectral peak.

Spectral surfing in SF-CARS is implemented by synchronizing two mechanically programmable components: the HWP that controls the SCG seed power and the delay stage that

controls the IFD being probed. Such synchronization requires information from both the CARS frequency calibration and the spectral surfing calibration functions. Fitting the *points of maximum spectral intensity* with a function yields the spectral surfing calibration function, $\theta(\Omega_R)$, where θ is the HWP angle, and Ω_R is the calculated Raman frequency or IFD. $\theta(\Omega_R)$ can simply follow a polynomial function or a set of piecewise-linear functions for more complicated datasets (as in this Letter). Figure 2(b) shows a simple algorithm to match the CARS frequency scan with the spectral surfing calibration function. As the delay stage moves during the CARS hyperspectral scan, $\Omega_R(x)$ can be calculated and then transformed to θ via the spectral surfing calibration function.

By using low SCG seed power, a Stokes supercontinuum can be generated that spans only a few key vibrational frequencies in the fingerprint, as shown in Fig. 2(c). By contrast, at much higher seed powers, the Stokes effectively spans the silent and CH/OH frequencies (2000–3500 cm^{-1}). However, with spectral surfing, an evolving supercontinuum can be generated that is higher in *effective* spectral intensity, compared with a given static spectrum. Figure 2(c) presents the Stokes spectra at the low (37 mW) and high (220 mW) coupled powers, and the surfed spectrum composed of the maxima of an experimentally obtained sequence of power-tuned spectra.

To demonstrate the efficacy of spectral surfing, proof-of-concept hyperspectral CARS images of a mixture of dimethyl sulfoxide (DMSO) and benzonitrile are obtained using static low-power, static high-power, and spectrally surfed Stokes supercontinua, as shown in Fig. 3(a). The low-power condition yields enhanced CARS contrast deep in the fingerprint, at the 670 cm^{-1} resonance in DMSO, but lacks contrast at both lower and higher CARS frequencies. The high-power condition shows strong contrast at 2220 cm^{-1} (benzonitrile) and at higher frequencies, but poor contrast for lower-frequency resonances in the fingerprint. For example, contrast for the 460 cm^{-1} resonance in benzonitrile is no longer observable with the high-power generation condition. With spectral surfing, CARS intensity and contrast are significantly improved across the extended CARS frequency range [Figs. 3(a) and 3(d)], allowing concurrent contrast in the deep fingerprint, silent, and CH/OH vibrational spectral ranges. As with SF-CARS implemented with static SCG Stokes, concurrent multimodal imaging is also enabled with spectral surfing. This is demonstrated in Figs. 3(b) and 3(c), where second-harmonic generation contrast from a cotton fiber is included. While not present in this particular sample, any TPEF signals are also concurrently collected on a separate epi-detector. The CARS images shown in Fig. 3 are raw and unmodified. However, because a full hyperspectral stack is collected, contrast can be further bolstered in such images by applying simple image processing that subtracts on-peak and off-peak (not shown) [22,23].

Because of the coherent mixing of the nonresonant background and vibrationally resonant signals, CARS spectra often appear distinct from spontaneous Raman spectra [1,15]. For the quantitative analysis that is so important to materials characterization, it is becoming commonplace to use post-acquisition spectral "retrieval" tools that convert raw CARS spectra to comparable Raman spectra [15]. Such retrieval algorithms are compatible with SF-CARS techniques, even when utilizing a highly structured Stokes supercontinuum [14,16,24]. We find that such a spectral retrieval is also

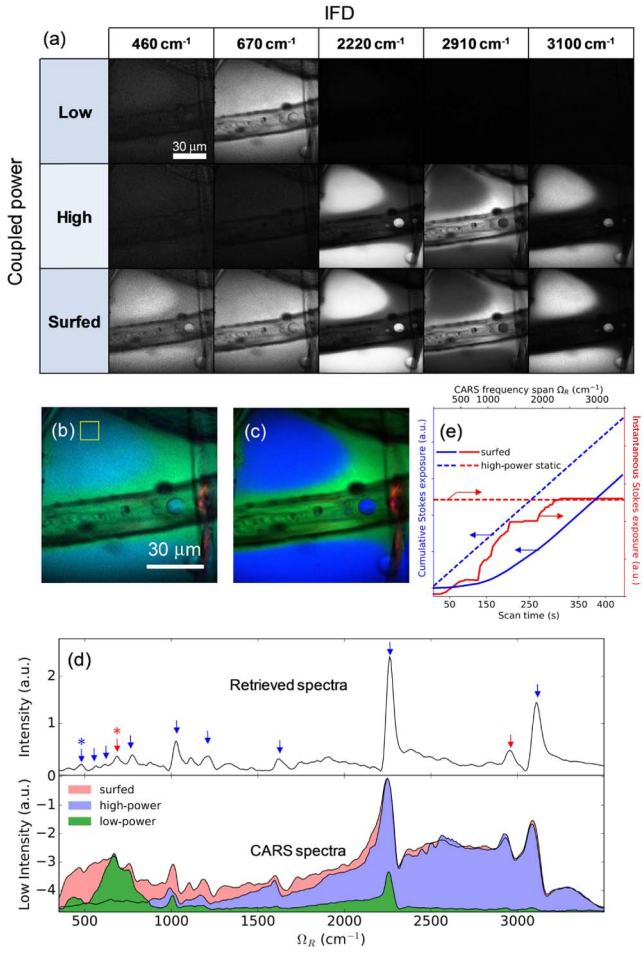

Fig. 3. CARS images, spectra, and Stokes exposure under "low," "high," and surfed conditions. (a) CARS images obtained at vibrational resonances corresponding to 460 cm^{-1}, 670, 2220, 2910, and 3100 cm^{-1} using low (37 mW) and high (220 mW) SCG seed powers, and with the spectrally surfed Stokes supercontinuum. For each column (frequency), the image display settings are identical, and were set by normalizing the surfed condition. (b) Multimodal image of the benzonitrile, DMSO, and a cellulose fiber mixture obtained from the surfed hyperspectra of (a) with 460 cm^{-1} (blue, benzonitrile), 670 cm^{-1} (green, DMSO), and second-harmonic signal (red). (c) Multimodal image from the surfed 2220 cm^{-1} (blue, benzonitrile), 2910 cm^{-1} (green DMSO), and second-harmonic signal (red). (d) CARS spectra (rolling average of four spectral points, ~20 cm^{-1}) obtained from the 20 × 20 pixel region of interest highlighted in (b), and the Raman-retrieved spectra of the "surfed" condition. The arrows point to known peaks of benzonitrile (blue) and DMSO (red). The two arrows marked with asterisks designate the frequencies used to compose the image in (b). (e) Sample exposure versus hyperspectral scan time. The blue curves are cumulative exposure, calculated by integrating in scan time the instantaneous (red curves) spectral intensity of the Stokes supercontinuum.

compatible with actively surfed CARS spectra. Despite the dynamically varying Stokes spectrum and, thus, the nonresonant background signal, Kramers–Kronig algorithms such as those provided by Camp *et al.* [15] are useful, as long as the acquired background signal used for retrieval is obtained with the same surfed protocol. As shown in Fig. 3(d), the

unprocessed CARS spectrum can be used to retrieve a Raman-like spectrum that better elucidates small vibrational signals deep into the fingerprint region.

The use of fixed blocks of glass means that the chirps of the pump and Stokes pulses cannot be identically matched across the entire CARS spectrum. With the experimental conditions reported here, the chirps are most matched in the low-frequency regime and, thus, the spectral resolution—simply measured as the FWHM of the benzonitrile peaks—increases steadily from 40 cm^{-1} deep in the fingerprint to 100 cm^{-1} at the OH frequencies. This implies a slight under-chirping of the Stokes at longer wavelengths. A more judicious choice of glass block lengths and further optimization of laser conditions would significantly improve the spectral resolution [14].

Commensurate with brighter CARS signals, spectral surfing has the added advantage of providing overall lower light exposures, an attribute that is particularly important in live cell and noninvasive tissue imaging applications [25,26]. By ramping up the total Stokes (supercontinuum) power over the course of a scan, lower net Stokes energy is incident on the sample compared to the typical static-Stokes approach [14]. During the course of the CARS hyperspectral scan, a weaker, but more efficient, dose of Stokes supercontinuum is used in the fingerprint regime. Upon reaching the CH/OH frequencies, a stronger supercontinuum is used, and the sample light exposure per unit time reaches the high power case. In Fig. 3(e), we show that for broad scans spanning the fingerprint and CH/OH regions, the overall sample Stokes exposure is reduced approximately by one-third when using surfed versus the typical static Stokes supercontinuum case. The sample's Stokes exposure will be further reduced whenever the CARS hyperspectral scan is performed exclusively in the fingerprint regime.

In summary, by synchronizing the pump-Stokes IFD with the power-tuning generation characteristics of a supercontinuum Stokes source, one can significantly boost the brightness and contrast of CARS hypermicroscopy signals. Such "spectral surfing" of a dynamically varying Stokes supercontinuum easily extends the utility of an inexpensive PCF source from one that is largely relegated to CARS imaging in the silent-to-CH/OH vibrational region to one that is useful across a much larger vibrational spectral regime. With spectral surfing, the CARS signal and contrast are improved across a spectral range greater than 3000 cm^{-1}. This method is furthermore compatible with available Raman retrieval algorithms that allow for more quantitative hypermicroscopy analysis relevant in materials science and biomedical imaging. Finally, such power tuning of the Stokes beam means that less overall light is needed for imaging—an attribute that is important for low-light dosage applications such as live cell analysis. While the application of spectral surfing is demonstrated within the context of spectral-focusing CARS microscopy, the technique may find future applications in related four-wave mixing techniques and other cross-phase modulation time-gated methods.

Funding. Natural Sciences and Engineering Research Council of Canada (NSERC) (418388-2012); Canada Research Chairs (CRC-NSERC-231086).

Acknowledgment. The authors thank Andrew Vreugdenhil and Jayme Stabler for technical assistance with Raman spectra and Emily Korfanty for developmental assistance with the motorized half-wave plate. J. Porquez would like to acknowledge the Ontario Trillium Scholarship program.

REFERENCES

1. C. L. Evans and X. S. Xie, Annu. Rev. Anal. Chem. **1**, 883 (2008).
2. C. H. Camp, Jr. and M. T. Cicerone, Nat. Photonics **9**, 295 (2015).
3. H. Tu, Y. Liu, D. Turchinovich, M. Marjanovic, J. K. Lyngsø, J. Lægsgaard, E. J. Chaney, Y. Zhao, S. You, W. L. Wilson, B. Xu, M. Dantus, and S. A. Boppart, Nat. Photonics **10**, 534 (2016).
4. L. Brückner, T. Buckup, and M. Motzkus, J. Opt. Soc. Am. B **33**, 1482 (2016).
5. K. Chen, T. Wu, H. Wei, and Y. Li, Opt. Lett. **41**, 2628 (2016).
6. I. Pope, W. Langbein, P. Watson, and P. Borri, Opt. Express **21**, 7096 (2013).
7. A. F. Pegoraro, A. Ridsdale, D. J. Moffatt, Y. Jia, J. P. Pezacki, and A. Stolow, Opt. Express **17**, 2984 (2009).
8. T. Hellerer, A. M. K. Enejder, and A. Zumbusch, Appl. Phys. Lett. **85**, 25 (2004).
9. R. C. Burruss, A. D. Slepkov, A. F. Pegoraro, and A. Stolow, Geology **40**, 1063 (2012).
10. T. T. Le, T. B. Huff, and J.-X. Cheng, BMC Cancer **9**, 42 (2009).
11. B. N. Toleutaev, T. Tahara, and H. Hamaguchi, Appl. Phys. B **59**, 369 (1994).
12. K. P. Knutsen, J. C. Johnson, A. E. Miller, P. B. Petersen, and R. J. Saykally, Chem. Phys. Lett. **387**, 436 (2004).
13. C. H. Camp, Jr., Y. J. Lee, J. M. Heddleston, C. M. Hartshorn, A. R. Hight Walker, J. N. Rich, J. D. Lathia, and M. T. Cicerone, Nat. Photonics **8**, 627 (2014).
14. J. G. Porquez, R. A. Cole, J. T. Tabarangao, and A. D. Slepkov, Biomed. Opt. Express **7**, 4335 (2016).
15. C. H. Camp, Y. J. Lee, and M. T. Cicerone, J. Raman Spectrosc. **47**, 408 (2016).
16. A. F. Pegoraro, A. D. Slepkov, A. Ridsdale, D. J. Moffatt, and A. Stolow, J. Biophotonics **7**, 49 (2014).
17. K. M. Hilligsøe, T. V. Andersen, H. N. Paulsen, C. K. Nielsen, K. Mølmer, S. Keiding, R. Kristiansen, K. P. Hansen, and J. J. Larsen, Opt. Express **12**, 1045 (2004).
18. J. M. Dudley, G. Genty, and S. Coen, Rev. Mod. Phys. **78**, 1135 (2006).
19. E. R. Andresen, V. Birkedal, J. Thøgersen, and S. R. Keiding, Opt. Lett. **31**, 1328 (2006).
20. I. Hartl, X. D. Li, C. Chudoba, R. K. Ghanta, T. H. Ko, J. G. Fujimoto, J. K. Ranka, and R. S. Windeler, Opt. Lett. **26**, 608 (2001).
21. T. Kamali, B. Považay, S. Kumar, Y. Silberberg, B. Hermann, R. Werkmeister, W. Drexler, and A. Unterhuber, Opt. Lett. **39**, 5709 (2014).
22. I. Rocha-Mendoza, W. Langbein, P. Watson, and P. Borri, Opt. Lett. **34**, 2258 (2009).
23. O. Burkacky, A. Zumbusch, C. Brackmann, and A. Enejder, Opt. Lett. **31**, 3656 (2006).
24. Y. Liu, M. D. King, H. Tu, Y. Zhao, and S. A. Boppart, Opt. Express **21**, 8269 (2013).
25. A. F. Pegoraro, A. Ridsdale, D. J. Moffatt, J. P. Pezacki, B. K. Thomas, L. Fu, L. Dong, M. E. Fermann, and A. Stolow, Opt. Express **17**, 20700 (2009).
26. B. G. Saar, R. S. Johnston, C. W. Freudiger, X. S. Xie, and E. J. Seibel, Opt. Lett. **36**, 2396 (2011).